Available online at www.sciencedirect.com
SCIENCE DIRECT®
International Journal of Heat and Mass Transfer 48 (2005) 4914–4925
International Journal of HEAT and MASS TRANSFER
www.elsevier.com/locate/ijhmt

Mathematical modelling and experimental investigation of tropical fruits drying

Md Azharul Karim [a,*], M.N.A. Hawlader [b]

[a] Department of Mechanical and Manufacturing Engineering, Faculty of Engineering, University of Melbourne, Melbourne VIC 3010, Australia
[b] Department of Mechanical and Manufacturing Engineering, National University of Singapore, 10 Kent Ridge Crescent, Singapore 119260, Singapore

Received 12 February 2004; received in revised form 31 January 2005
Available online 8 August 2005

Abstract

A mathematical model has been developed to solve the heat and mass transfer equations for convective drying of tropical fruits. The model takes into account shrinkage of material and moisture content and shrinkage dependant effective diffusivity. Heat and mass transfer equations for the dryer, termed as equipment model, have also been developed to determine the changes of drying potential of the drying medium during drying. The material model is capable of predicting the instantaneous temperature and moisture distribution inside the material. The equipment model, on the other hand, describes the transfer process in the tunnel dryer and predicts the instantaneous temperature and humidity ratio of air at any location of the tunnel. Thus, the model is capable of predicting the dynamic behaviour of the dryer. The predicted results were compared with experimental data for the drying of banana slices dried in a solar dryer. Experimental results validated the model developed.

Keywords: Drying; Mathematical model; Shrinkage; Experimental validation

1. Introduction

The drying of fruit and vegetables is a subject of great importance. Dried fruit and vegetables have gained commercial importance and their growth on a commercial scale has become an important sector of the agricultural industry. Lack of proper processing causes considerable damage and wastage of seasonal fruits in many countries, which is estimated to be 30–40% in developing countries. It is necessary to remove the moisture content of fruits to a certain level after harvest to prevent the growth of mould and bacterial action.

Theoretical studies on drying started based on pure mass transfer, neglecting the heat transfer and its effect on drying, thus assuming that mass transfer only occurs by diffusion and capillary action. To date, considerable research has been conducted beyond this simplified model. Many mathematical models have been proposed to describe the drying processes [1–3]. Reviews of the different mathematical models have been presented by Rossen and Hayakawa [4] and Fortes and Okos [5]. Upon drying (loss of water) this volume change is

* Corresponding author. Tel.: +613 8344 6756; fax: +613 9347 8784.
E-mail address: makarim@mame.mu.oz.au (M.A. Karim).

0017-9310/$ - see front matter © 2005 Elsevier Ltd. All rights reserved.
doi:10.1016/j.ijheatmasstransfer.2005.04.035

Nomenclature

b	half thickness of drying specimen (m)
c	specific heat (J/kg K)
c_{pa}	specific heat of air (J/kg K)
D	diffusion coefficient (m^2/s)
G_o	air mass flux (kg/m^2 s)
h	convective heat transfer coefficient (W/m^2 K)
h_{fg}	enthalpy of evaporation (J/kg)
h_m	mass transfer coefficient (m/s)
k	thermal conductivity (W/m K)
L	thickness of the drying specimen (m)
M	moisture content of specimen (g/g dry)
N	moisture flux (kg/m^2s)
Nu	Nusselt number
Pr	Prandlt number
Re	Reynolds number
RH	relative humidity
Sc	Smith number
Sh	Sherwood number
t	time (s)
T	temperature (°C)
u	shrinkage velocity (m/s)
x	distance from the centre of the drying specimen (m)
z	distance from the inlet of the dryer (m)
Y	air humidity ratio (kg/kg dry air)
Z	length of the dryer (m)
ρ	density (kg/ m^3)
ε	bed void fraction (dimensionless)

Subscripts

0	initial, reference
a	air
d	drying
e	equilibrium
eff	effective
m	material (banana sample)
ref	reference
s	solid, surface, shrinkage
w	water

expressed as shrinkage. This shrinkage phenomenon changes the heat and mass exchange area and affects in particular the diffusion coefficient of the material, which is one of the main parameters governing the drying process [6,7].

Theoretical and experimental studies were carried out to analyze and foresee the mass transfer in foodstuffs [8–12]. However, few works were carried out on the drying kinetics taking into account the shrinkage phenomenon [13,6]. These works however pointed out that the shrinkage phenomenon has a strong influence on the drying rate.

Although considerable studies have been performed on the drying of agricultural products, reliable simulation models to aid the design of tunnel dryers for fruits are few. The majority of the models developed have not considered the 'equipment model', which expresses the effect of heat and mass transfer in the material on the drying medium. It is vital to know the effect of heat and mass transferred from the material to the drying medium for designing a dryer for a particular task.

A reliable dryer model, which can express accurately the drying kinetics of the product as well as predict the drying behaviour of the air and the materials to be dried, is often needed. This type of model can be used as a design tool for batch type tunnel dryer.

In this study, a simulation model describing simultaneous heat and mass transfer processes is proposed to describe the drying potential of foodstuffs. The model takes shrinkage of material during drying into consideration. Extensive experiments were conducted using bananas as a sample to compare the experimental results with simulation results for validation purpose.

2. Drying model formulation

The modelling of the dryer comprises both material and equipment models. The material model determines the drying kinetics and the equipment model determines the changes of the condition of the drying medium with time and space during drying. The material model together with the equipment model constitutes a complete modelling tool for a batch type tunnel dryer, which is capable of predicting the dynamic behaviour of the dryer.

2.1. Material model

In the present model, it is assumed that moisture transport occurs by diffusion in only one direction—from the interior to the air–sample interface, and evaporation takes place at the interface. Shrinkage of agricultural products during drying is an observable physical phenomenon, which occurs simultaneously with moisture diffusion.

The drying of shrinking material involves coupling between drying processes and deformation. In vegetables and fruits, the volume of shrinkage is very close to the volume of water loss by dehydration [14]. To simplify the model, the following assumptions were made:

1. Moisture movement and heat transfer are one dimensional;
2. No chemical reaction takes place during drying i.e. thermal and chemical properties of material, air and moisture are constant within the range of temperatures considered;
3. The material undergoes shrinkage as drying progresses;
4. Drying air is distributed uniformly through the dryer.

The drying material is considered as a thin slab of thickness $L = 2b$ at a uniform initial temperature T_0 and moisture content M_0. The two sides are exposed to an air flow at temperature T_a and relative humidity RH. If it is considered that material surface shrinks at a velocity $u(x)$ towards the centre of the material sample, the shrinkage effect can be considered as analogous to convective flow [15]. The shrinkage effect appears explicitly in terms of convective velocity in the heat and mass transfer equations [15].

2.1.1. Mass transfer equation

To develop the mass transfer equations, consider a control volume of the drying material with thickness dx. The conservation of mass equations for the control volume (CV) can be expressed as:

(Moisture gained in CV − Moisture out of CV) + generation = storage

Net change in moisture in CV due to diffusion

$$= (N''_x A - N''_{x+\mathrm{d}x} A) = N''_x A - \left[N''_x A + A\frac{\partial (N''_x)}{\partial x}\mathrm{d}x\right]$$

$$= -A\frac{\partial}{\partial x}(N''_x)\mathrm{d}x = (A\,\mathrm{d}x)\rho D\frac{\partial^2 M}{\partial x^2} \tag{1}$$

Similarly, net moisture gain for shrinkage can be expressed as:

$$= N''_{s,x} A - N''_{s,x+\mathrm{d}x} A = \rho u M A - \rho (M + \Delta M) u A$$

$$= -\rho u A \Delta M \tag{2}$$

$$\text{The moisture storage in CV} = \rho A\,\mathrm{d}x\frac{\partial M}{\partial t} \tag{3}$$

As it is considered that no chemical reaction occurs during drying, the generation term becomes zero. Combining Eqs. (1)–(3), conservation of mass equation can be written as:

$$A\,\mathrm{d}x\rho D\frac{\partial^2 M}{\partial x^2} - \rho \Delta M u A = \rho A\,\mathrm{d}x\frac{\partial M}{\partial t}$$

$$\therefore \frac{\partial M}{\partial t} + u\frac{\partial M}{\partial x} = D\frac{\partial^2 M}{\partial x^2} \tag{4}$$

2.1.2. Heat transfer equation

The equation for conservation of energy can be written as:

(Energy gained in CV − Energy out of CV) + generation = Energy storage

It is possible to derive the equation for differential energy balance in a similar fashion to mass balance. The final form of the equation is as follows:

$$\frac{\partial T}{\partial t} + u\frac{\partial T}{\partial x} = \alpha\frac{\partial^2 T}{\partial x^2} \tag{5}$$

For the materials undergoing shrinkage, diffusion coefficient D in Eq. (4) is not constant [16] but varies with moisture content. One way to solve the problem of the shrinkage effect is to incorporate the volume change into the diffusion coefficient. Therefore, to consider the real condition, an effective diffusion coefficient (D_{eff}) is introduced. Thus the actual equation that describes the diffusion of moisture in the material is given by

$$\frac{\partial M}{\partial t} + u\frac{\partial M}{\partial x} = D_{\mathrm{eff}}\frac{\partial^2 M}{\partial x^2} \tag{6}$$

D_{eff} can be calculated from the following equation [16]:

$$\frac{D_{\mathrm{ref}}}{D_{\mathrm{eff}}} = \left(\frac{b_0}{b}\right)^2 \tag{7}$$

where D_{ref}, reference diffusion coefficient, is determined experimentally. The thickness ratio is obtained from the following equation [17]:

$$b = b_0\left[\frac{\rho_w + \overline{M}\rho_s}{\rho_w + \overline{M}_0\rho_s}\right] \tag{8}$$

It is necessary to determine the shrinkage velocity in order to solve the governing equations. At present, as the shrinkage velocity cannot be predicted and experimental determination is also difficult [18], an assumption on shrinkage velocity has to be made. This study assumes a linear distribution of shrinkage velocity. Thus at any point in the sample, shrinkage velocity can be expressed as [18]:

$$u(x) = u(b)\frac{x}{b} \tag{9}$$

and the velocity at the exposed surface is:

$$u(b) = \frac{b - b(\mathrm{old})}{\Delta t} \tag{10}$$

The moisture content throughout the specimen is assumed to be uniform at the beginning of drying. In the middle of the specimen, $x = 0$, the moisture gradient is considered zero. The initial and boundary conditions of Eqs. (5) and (6) are given below:

The initial conditions are: $M|_{t=0} = M_0$, $T|_{t=0} = T_0$.

Boundary conditions:

$$\text{at } x = 0, \quad \left.\frac{\partial M}{\partial x}\right|_{x=0} = 0 \quad \text{and} \quad \left.\frac{\partial T}{\partial x}\right|_{x=0} = 0$$

and at $x = b$, moisture balance can be written as:

$$-D_{\text{eff}}\left.\frac{\partial M}{\partial x}\right|_{x=b} + uM|_{x=b} = h_{\text{m}}(M - M_{\text{e}})|_{x=b}. \tag{11}$$

Energy balance at the boundary, $x = b$ can be expressed as:

$$\left(k\frac{\partial T}{\partial x} - \rho c_p u T\right)\Big|_{x=b} = h(T_{\text{a}} - T)|_{x=b} - h_{\text{m}}\rho(M - M_{\text{e}})h_{\text{fg}}|_{x=b} \tag{12}$$

Mass transfer coefficient, h_{m} can be determined from the following relationships [19] for laminar flow (Eq. (13)) and turbulent flow (Eq. (14)), respectively:

$$Sh = \frac{h_{\text{m}}L}{D_0} = 0.332Re^{0.5}Sc^{0.33} \tag{13}$$

and

$$Sh = \frac{h_{\text{m}}L}{D_0} = 0.0296Re^{4/5}Sc^{1/3} \tag{14}$$

Similarly, the heat transfer coefficient can be calculated from the following relationships for laminar (Eq. (15)) and turbulent (Eq. (16)) flow, respectively:

$$Nu = \frac{hL}{k} = 0.332Re^{0.5}Pr^{0.33} \tag{15}$$

$$Nu = \frac{hL}{k} = 0.0296Re^{0.5}Pr^{0.33} \tag{16}$$

2.2. Equipment model

In obtaining a set of differential equations to describe changes in the drying medium during drying, the following assumptions were made:

1. Thermal properties of moisture and air are constant;
2. The problem is one dimensional and conduction heat transfer within the bed is negligible;
3. The changes in void fraction or bed porosity are negligible;
4. Sample (product) size is uniform;
5. Product is uniformly distributed in the drying chamber.

2.2.1. Energy balance

To determine the energy balance equation for the dryer, consider a control volume of the dryer, of thickness dz, at a distance z from the inlet of the dryer. The change of energy in air across the control volume can be written as:

$$G_0 c_{\text{pa}}\frac{\partial T_{\text{a}}}{\partial z}\mathrm{d}z\,\mathrm{d}t \tag{17}$$

The amount of air within the elemental control volume is $\varepsilon\rho_{\text{a}}\mathrm{d}z$. The change of energy in the air of the control volume during time dt is:

$$\varepsilon\rho_{\text{a}}\mathrm{d}z\,c_{\text{pa}}\frac{\partial T_{\text{a}}}{\partial t}\mathrm{d}t \tag{18}$$

As described earlier, the material temperature change along the dryer has been neglected. The sensible heat change of material due to the change in temperature with time is:

$$(1-\varepsilon)\rho_{\text{s}}\frac{\partial T_{\text{s}}}{\partial t}(c_{\text{s}} + c_{\text{w}}M)\mathrm{d}z\,\mathrm{d}t \tag{19}$$

The energy required for evaporation of moisture from the material is:

$$h_{\text{fg}}\frac{\partial M}{\partial t}\rho_{\text{s}}(1-\varepsilon)\mathrm{d}z\,\mathrm{d}t \tag{20}$$

Taking the energy balance between air and material, the energy balance equation can be written as:

$$\begin{aligned} -G_0 c_{\text{pa}}\frac{\partial T_{\text{a}}}{\partial z}\mathrm{d}z\,\mathrm{d}t = {} & \varepsilon\rho_{\text{a}}\mathrm{d}z\,c_{\text{pa}}\frac{\partial T_{\text{a}}}{\partial t}\mathrm{d}t \\ & + (1-\varepsilon)\rho_{\text{s}}\frac{\partial T_{\text{s}}}{\partial t}(c_{\text{s}} + c_{\text{w}}M)\mathrm{d}z\,\mathrm{d}t \\ & - h_{\text{fg}}\frac{\partial M}{\partial t}\rho_{\text{s}}(1-\varepsilon)\mathrm{d}z\,\mathrm{d}t \end{aligned} \tag{21}$$

2.2.2. Mass balance

The change in humidity of the air leaving the control volume is:

$$G_0\left(\frac{\partial Y}{\partial z}\right)\mathrm{d}z\,\mathrm{d}t \tag{22}$$

Increase in water content in the air over time dt (storage) is:

$$\varepsilon\rho_{\text{a}}\frac{\partial Y}{\partial t}\mathrm{d}t\,\mathrm{d}z \tag{23}$$

Water evaporated from the material is:

$$\rho_{\text{s}}(1-\varepsilon)\frac{\partial M}{\partial t}\mathrm{d}t\,\mathrm{d}z \tag{24}$$

Moisture balance equation can be written as:

$$G_0\frac{\partial Y}{\partial z}\mathrm{d}z\,\mathrm{d}t + \varepsilon\rho_{\text{a}}\frac{\partial Y}{\partial t}\mathrm{d}t\,\mathrm{d}z = -\rho_{\text{s}}(1-\varepsilon)\frac{\partial M}{\partial t}\mathrm{d}t\,\mathrm{d}z \tag{25}$$

$$\therefore G_0\frac{\partial Y}{\partial z} + \varepsilon\rho_{\text{a}}\frac{\partial Y}{\partial t} = -\rho_{\text{s}}(1-\varepsilon)\frac{\partial M}{\partial t} \tag{26}$$

Under conditions generally occurring in practice, the time derivatives $\frac{\partial T_{\text{a}}}{\partial t}$ and $\frac{\partial Y}{\partial t}$ are negligible in comparison to their space derivatives [20]. In most practical cases it can therefore be expected that a good approximation will still be obtained if the time derivatives of Eqs. (21) and (26) are neglected.

Hence Eqs. (21) and (26) can be written as:

$$-\frac{G_0 c_{pa}}{\rho_s(1-\varepsilon)}\frac{\partial T_a}{\partial z}=\frac{\partial T_s}{\partial t}(c_s+c_w M)-\frac{\partial M}{\partial t}h_{fg} \quad (27)$$

and

$$G_0\frac{\partial Y}{\partial z}=-\rho_s(1-\varepsilon)\frac{\partial M}{\partial t} \quad (28)$$

The initial and boundary conditions are

- at $x=0$ and $t=0$; $T_a=T_0, \mathrm{d}T_a/\mathrm{d}t=0$ and $Y=Y_0$, $\mathrm{d}Y/\mathrm{d}t=0$,
- at $x>0, t=0$; $T_a=T_0, Y=Y_0$.

The above equipment model together with the material model developed earlier constitutes a complete modelling tool for a batch type tunnel dryer.

2.2.3. Method of solution

The governing differential equations describing drying characteristics and dryer behaviour were solved numerically. Physical properties of banana, the fruit considered in this study, were taken from references [21] and [22]. Diffusion coefficient, initial moisture content, equivalent moisture content and shrinkage of the sample were determined experimentally. A computer program in FORTRAN was developed to solve the set of finite difference equations.

3. Materials and methods

In order to conduct drying experiments, a batch type solar cabinet dryer was built with an auxiliary heater. The details of this dryer can be found in reference [23]. The temperatures were measured using T-type thermocouples. All thermocouples were calibrated using standard thermometers and connected to a data logger. Relative humidity at the inlet and outlet were measured by a humidity transmitter, which gave a voltage reading proportional to the relative humidity. A reading of 1–5 volts represented 0–100% relative humidity.

The weight of the material during drying was continuously measured using a load cell, which was calibrated using standard weights. During the experiments, it was found that airflow in the dryer affected the reading of the load cell and differed from the reading under stable conditions. The load cell was therefore calibrated for each air velocity considered in this study by placing the load cell in the dryer section. Thus, for each velocity there was a different calibration for the load cell. Airflow rate was calculated by measuring the air velocity at the entrance of the dryer section using a calibrated hot wire anemometer. The surface temperature of the material was measured by installing a 'wall-mount' type thermocouple on the sample surface. Air flow rate was varied by controlling the speed controller of the blower fan. The air temperature was varied using a temperature controller attached to the auxiliary heater.

Fresh, ripe bananas of approximately the same size were used in the drying tests. Banana slices were prepared first by peeling the skin and then slicing in to 4 mm thickness and approximately the same diameter. Diameters of the specimens varied between 30 and 36 mm. The slices were then uniformly spread onto five plastic mesh trays. Plastic mesh was selected because of its poor thermal conductivity relative to metal mesh. Each run included approximately 600 g of material. After the dryer had reached the steady state condition for the set parameters, the set of trays with specimen were placed inside the drying chamber and measurement started. The door of the dryer was properly closed and sealed to ensure no leakage of hot air.

During the course of the experiment, material and air temperatures, relative humidity, air velocity and material weight were monitored using a 16 channel data logger at one-minute intervals during the first hour of drying and at 5–15 min intervals from the next hour onwards. Initial moisture content was about 4.0 g/g dry and final moisture content was between 0.22 and 0.32 g/g dry. The thickness of the material was measured at one-hour intervals to monitor the shrinkage of the material. Experiments continued until the final desired moisture content was achieved or no change in material weight was observed for at least half an hour. After each drying test, the specimens were dried in an oven at 100 °C for at least 24 h to obtain the bone-dry mass of the material and to determine the moisture content of

Table 1
Drying air and material (banana) properties

Drying air property and drying conditions						Material properties	
Drying temperature, °C	Relative humidity, %	Specific heat of air, J/kg K	Density of air, kg/m^3	Enthalpy of evaporation, J/kg	Thermal conductivity of air W/m K	Density of banana, kg/m^3	Initial moisture content, g/g dry
60	15	1005.04	1.073	2358600	0.0287	980	4
50	22	1004.38	1.106	2383000	0.0287	980	4
40	38	1003.72	1.141	2407000	0.0287	980	4

the original material. The average bone-dry mass was 20% of the original mass, which means that fresh banana contains about 80% water.

Experiments were conducted at different air flow rates and temperatures. Air velocity was varied from 0.3 m/s to 0.7 m/s and temperature was varied from 40 to 60 °C. The variables considered for this experiment are shown in Table 1.

Drying air properties, material (banana) properties and experimentally determined initial moisture contents are also presented in Table 1.

4. Results and discussion

4.1. Effective diffusion coefficient

The diffusion coefficient for each drying condition was determined from experimental data using the following widely used equation:

$$\ln\frac{M}{M_0} = \ln(8/\pi^2) - \pi^2 Dt/L^2 \tag{29}$$

When the experimental values of $\ln M/M_0$ are plotted against t/L^2, the slope of the curve is a measure of effective diffusivity. Fig. 1 shows such a plot for the drying of banana at 50 °C and 0.7 m/s air velocity. It can be seen that the slope of the curve, i.e. diffusivity decreases as the drying progresses. This is expected as the shrinkage and hardening of the material offer increasing resistance to moisture diffusion. This result differs from the results reported by Hawlader et al. [24] for tomato drying. They reported an increasing slope of the curve, hence increasing diffusivity towards the end of drying.

In Eq. (29), the thickness L was assumed to be constant throughout the drying process. However, experiments and literature show that the thickness of a sample is not constant, but shrinks significantly. For example, in one of the present experiments the final thickness of banana was 1.13 mm, which is 29% of the initial thickness. To take this shrinkage into account, Eq. (7) was used to obtain the effective diffusivity throughout the drying process. The diffusivity calculated from Eq. (29) was considered as the reference diffusivity. To find the reference diffusivity, only the straight portion of the $\ln M/M_0$ vs t/L^2 curve was considered [24]. Experimentally determined reference diffusion coefficients of banana at the different drying conditions considered in this study are presented in Table 2.

4.2. Drying characteristics

Fig. 2 shows the experimental and predicted variation of moisture content of material with time at air temperature 60 °C and velocity 0.3 m/s. In simulation, moisture content of the material at any time step was determined by averaging the calculated moisture distribution in the sample. From the drying curves, it can be seen that no constant drying rate period is evident. The predicted and experimental results show very close agreement.

4.2.1. Moisture distribution in material during drying

In the drying operation, it is important to know the temperature and moisture distribution in the material and its change during drying; the present mathematical model developed is able to predict this. The predicted moisture distribution within the sample as a function of thickness during drying at air temperature 40 °C air velocity 0.7 m/s is presented in Fig. 3. Since it is difficult to determine the moisture distribution within a sample experimentally [25] moisture distribution inside the material was not measured in the present study. Only the overall (average) moisture content was determined

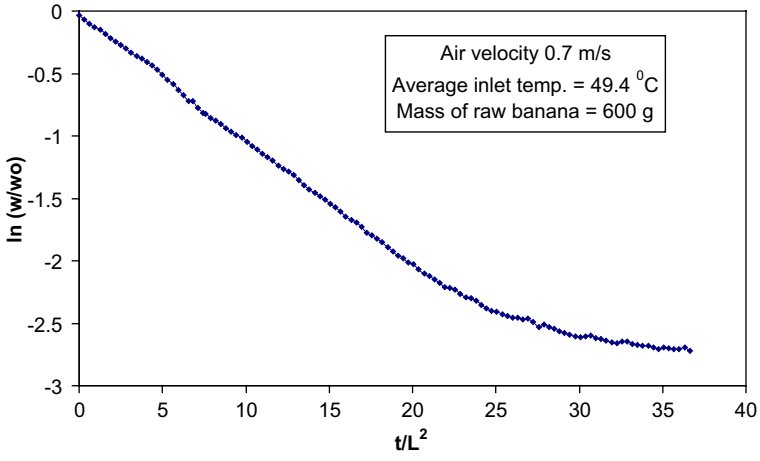

Fig. 1. Plot of $\ln M/M_0$ versus t/L^2.

Table 2
Diffusion coefficients of banana drying at different drying conditions

Air velocity, m/s	Temperature, °C	Diffusion coefficient, m^2/s
0.7	60	2.41×10^{-10}
	50	1.74×10^{-10}
	40	9.8×10^{-11}
0.5	60	2.23×10^{-10}
	50	1.61×10^{-10}
	40	7.33×10^{-11}
0.3	60	1.95×10^{-10}
	50	1.57×10^{-10}
	40	6.61×10^{-11}

experimentally. However, to compare with the experimental results, predicted average moisture content of the entire sample was calculated. Respective experimental and predicted average moisture contents are also presented in Fig. 3.

No evidence of constant drying rate period can be found in the drying curves presented in this figure. It can be seen that the surface directly exposed to the drying air approached the equilibrium moisture content faster and the changes in the deeper layers of materials are slow. The predicted and experimental results show reasonably close agreement, which validates the model developed to express drying characteristics. Other tests considered in this study also showed similar results.

4.2.2. Material temperature distribution

The surface temperature of the materials was recorded continuously during drying. Using the computer program, the temperature was predicted at different locations from the centre of the material. Fig. 4 shows

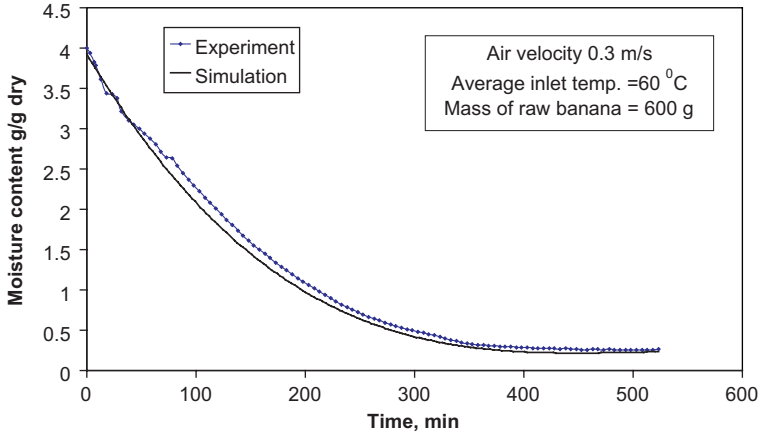

Fig. 2. Experimental and predicted variation of moisture content with time at temperature 60 °C and air velocity 0.3 m/s.

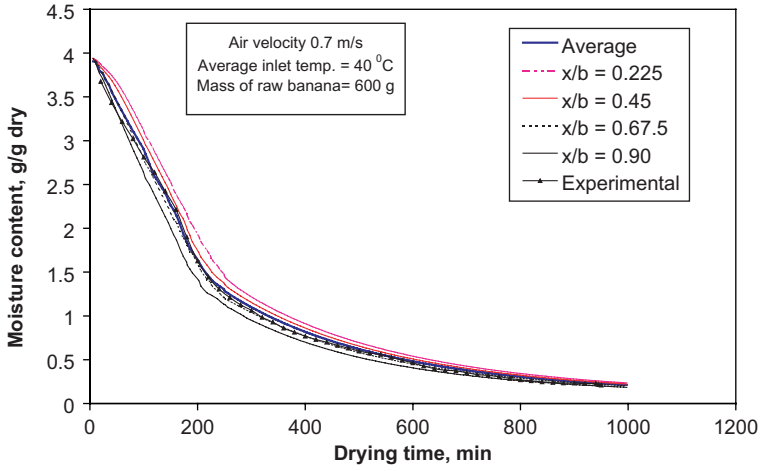

Fig. 3. Moisture profile of material during drying ($T_a = 40$ °C; air velocity = 0.7 m/s).

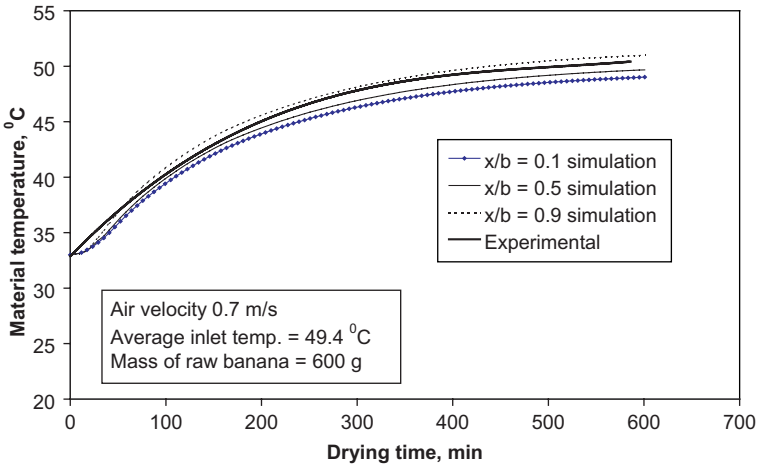

Fig. 4. Temperature distributions in material during drying with time ($T_a = 49.4$ °C; air velocity = 0.7 m/s).

the predicted temperature distribution inside the material with time at air velocity of 0.7 m/s and temperature 50 °C. The respective experimental surface temperature was also plotted on the same graph. The predicted surface temperatures agreed reasonably well with those obtained from experiment.

4.2.3. Experimental drying rate with time and moisture content

Figs. 5 and 6 present the experimental variation of drying rate as a function of moisture content and drying time respectively at air velocity 0.7 m/s with temperature as a variable. It can be seen that the drying rate is not constant throughout the drying period. It constantly drops until the equivalent moisture content of the product is reached. From Fig. 6, it is evident that the drying rate falls sharply at higher temperatures compared to lower temperatures.

Figs. 7 and 8 show the experimental variation of drying rate as a function of moisture content and drying time respectively at air temperature 60 °C with air velocity as a variable. From these figures it is evident that air temperature and air velocity have great effect on drying rates. If the drying rates change found in Fig. 8 are compared with those shown in Fig. 6, it can be concluded that drying rate is stronger function of temperature than that of air velocity. Initial drying rate was increased from 0.0132 g/(g dry-min) to 0.0321 g/(g dry-min) for increasing air temperature from 40 °C to 60 °C. On the other hand, drying rate was increased from 0.0286 g/(g dry-min) to 0.0321 g/(g dry-min) for increasing air velocity from 0.3 m/s to 0.7 m/s at 60 °C.

The relationship between drying rate and moisture content at different drying temperatures and velocities is presented in Table 3. From these equations it is possible to estimate the drying rate at any condition of moisture content of the material. The relationship between drying rate and drying time at different air velocities and temperatures are shown in Table 4. Drying time required can be estimated from these equations. In these equations d_m and d_t indicated the relationship of drying rate with moisture content and drying time respectively.

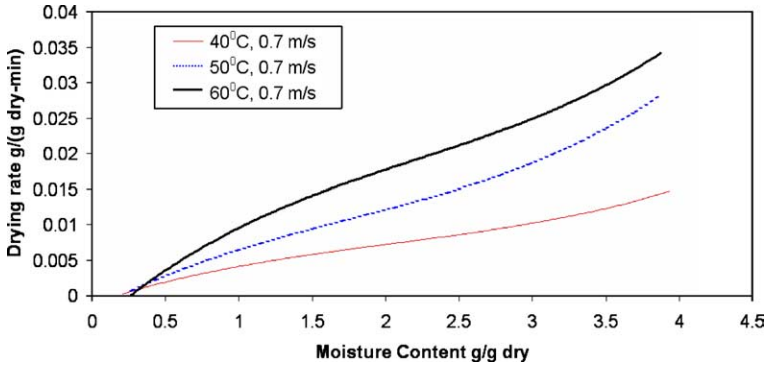

Fig. 5. Drying rate versus moisture content at air temperatures 40, 50 and 60 °C, and air velocity 0.7 m/s.

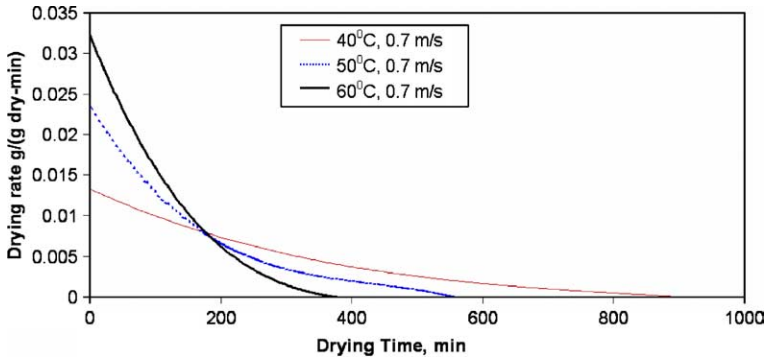

Fig. 6. Drying rate versus drying time at air temperatures 40, 50 and 60 °C, and air velocity 0.7 m/s.

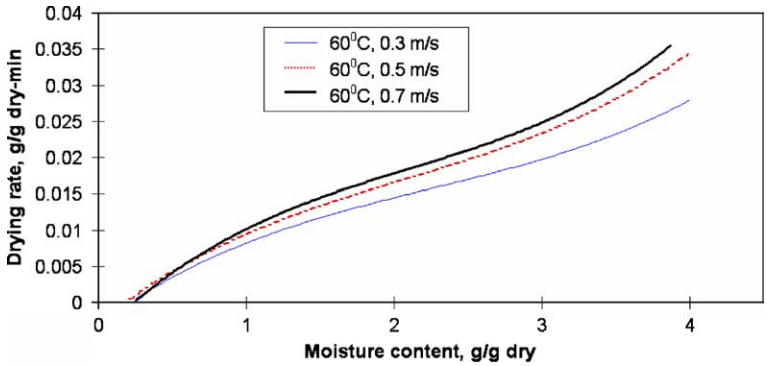

Fig. 7. Drying rate versus moisture content at air velocities 0.3, 0.5 and 0.7 m/s, and temperature 60 °C.

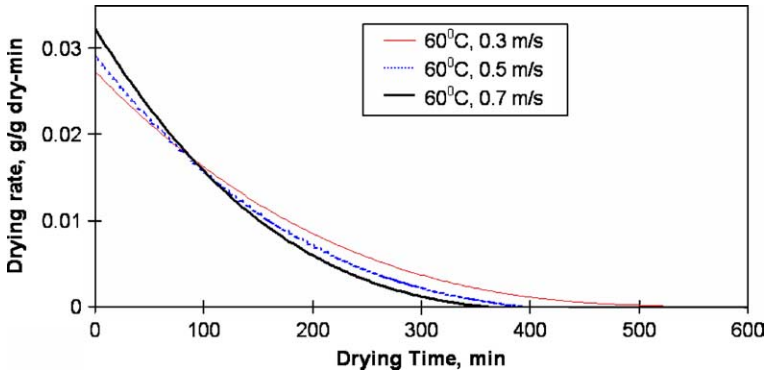

Fig. 8. Drying rate versus drying time at air velocities 0.3, 0.5 and 0.7 m/s, and temperature 60 °C.

4.3. Dryer characteristics

Fig. 9 shows the temperature distribution of drying air along the dryer. In the experiment, dryer temperatures at the inlet and outlet were recorded throughout the drying period. However, from the simulation program, the temperature variation at different locations of the dryer with time was computed. In this way, the dryer outlet temperature was predicted. The predicted outlet temperatures are compared with measured temperatures for different drying conditions.

In a batch type tunnel dryer, air humidity increases as it passes through the dryer. The humidity ratio of the drying air at different locations of the dryer with time was determined with the simulation program. Relative humidity of air at the inlet and outlet were measured in the experiments. In Fig. 10, the predicted humidity ratio distribution along the dryer with time is presented.

Table 3
Relationships between drying rate and moisture content at different drying conditions

Velocity, m/s	Temperature, °C	Relationship between drying rate and moisture content
0.3	40	$d_m = 0.0003M^3 - 0.0021M^2 + 0.0065M - 0.0018$
	50	$d_m = 0.0005M^3 - 0.0039M^2 + 0.0125M - 0.0025$
	60	$d_m = 0.0006M^3 - 0.0044M^2 + 0.0148M - 0.0029$
0.5	40	$d_m = 0.0003M^3 - 0.0017M^2 + 0.006M - 0.0012$
	50	$d_m = 0.0005M^3 - 0.0028M^2 + 0.0086M - 0.0015$
	60	$d_m = 0.0008M^3 - 0.0049M^2 + 0.0163M - 0.0028$
0.7	40	$d_m = 0.0003M^3 - 0.0021M^2 + 0.0069M - 0.0011$
	50	$d_m = 0.0006M^3 - 0.0034M^2 + 0.0114M - 0.0022$
	60	$d_m = 0.0008M^3 - 0.0054M^2 + 0.0187M - 0.0045$

Table 4
Relationships between drying rate and time at different drying conditions

Velocity, m/s	Temperature, °C	Relationship between drying rate and drying time
0.3	40	$d_t = 6E - 12t_d^3 - 3E - 09t_d^2 - 1E - 05t_d + 0.0085$
	50	$d_t = -1E - 11t_d^3 + 5E - 08t_d^2 - 6E - 05t_d + 0.0193$
	60	$dR = -1E - 10t_d^3 + 2E - 07t_d^2 - 0.0001t_d + 0.0274$
0.5	40	$d_t = -3E - 12t_d^3 + 2E - 08t_d^2 - 2E - 05t_d + 0.0109$
	50	$d_t = -9E - 11t_d^3 + 1E - 07t_d^2 - 9E - 05t_d + 0.0215$
	60	$d_t = -2E - 10t_d^3 + 3E - 07t_d^2 - 0.0002t_d + 0.0291$
0.7	40	$d_t = -1E - 11t_d^3 + 3E - 08t_d^2 - 4E - 05t_d + 0.0133$
	50	$d_t = -2E - 10t_d^3 + 3E - 07t_d^2 - 0.0001t_d + 0.0235$
	60	$d_t = -3E - 10t_d^3 + 4E - 07t_d^2 - 0.0002t_d + 0.0324$

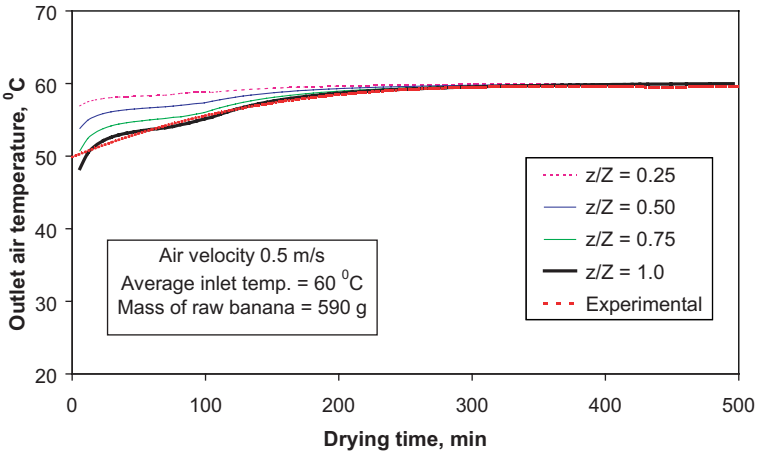

Fig. 9. Predicted and experimental temperature distribution along the dryer with time, $T_a = 60$ °C and air velocity = 0.5 m/s.

The measured outlet humidity ratio is also plotted for comparison. The reasonable agreement in both temperature (Fig. 9) and humidity (Fig. 10) distribution validates the material model and related assumptions. It can be seen in Fig. 10 that at the beginning, humidity ratio of outlet air increases. A possible reason for this phenomenon is the presence of some free water on the specimen surface. It can also be seen that the increase is higher in the simulation compared to the experiments. In the simulation, heat conduction and heat loss in the dryer is considered negligible. However in practice, there will be heat consumption by the trays at the beginning, heat loss through the walls of the drying chamber and heat loss from the dryer when the

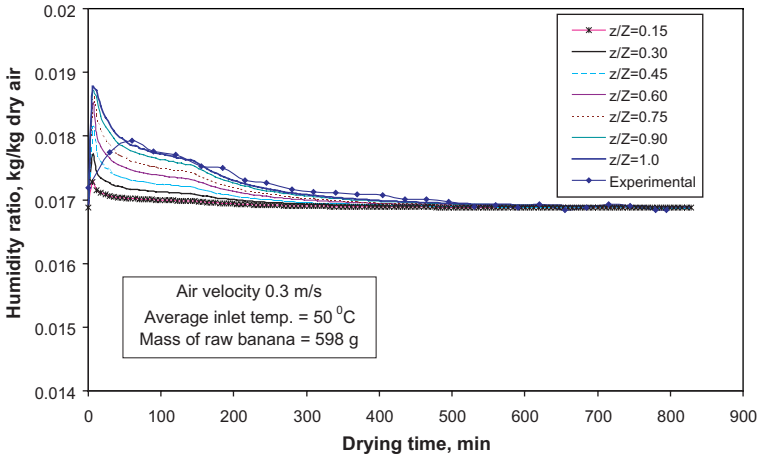

Fig. 10. Experimental and predicted dryer outlet air humidity ratio with time, $T_a = 50$ °C and air velocity = 0.3 m/s.

door is opened to place the trays. If these factors are considered, it is understandable that experimental moisture removal at the beginning will be lower than the ideal.

As this model is able to estimate the condition of drying air at any location of the dryer, it is possible to determine the effective length of the drying chamber and recirculation points.

5. Conclusions

In this investigation a mathematical model for fruit drying has been developed which gives accurate predictions of drying and dryer characteristics. Although the model developed is mathematically simple, it is able to provide reliable predictions of the drying rate and temperature and moisture distribution in the material, and temperature and moisture distributions in the drying air along the dryer during the drying process. Experiments were conducted using banana samples to evaluate the results predicted by the model. As both the material and equipment models agreed closely with the experimental values, the mathematical formulations and the related assumptions are considered reliable to predict the performance of dryers. Empirical drying rate equations are developed. These equations will be helpful to estimate the drying rate at any moisture condition of the material and to estimate the drying time for a particular task.

References

[1] I. Turner, A.S. Mujumdar, Mathematical Modelling and Numerical Techniques in Drying Technology, Marcel Dekker Inc., New York, 1997.

[2] T.Z. Harmathy, Simultaneous moisture and heat transfer in porous systems with particular reference to drying, Ind. Eng. Chem. Fundament. 8 (1969) 92–103.

[3] M.D. Mikhailov, Exact solution of temperature and moisture distribution in a porous half-space with moving evaporation front, Int. J. Heat Mass Transfer 18 (1975) 797–804.

[4] T.L. Rossen, K. Hayakawa, Simultaneous heat and mass transfer in dehydrated food, a review of theoretical models, In: AICHE Symp., V73, Vol. 163, 1977, pp. 71–86.

[5] M. Fortes, M.R. Okos, Drying theories: their bases and limitations as applied to foods and grains, in: A.S. Mujumdar (Ed.), Advances in Drying, Vol. 1, Hemisphere, Washington D.C., 1980, pp. 119–154.

[6] A.G.B. Lima, M.R. Queiroz, S.A. Nebra, Simultaneous moisture transport and shrinkage during drying solids with ellipsoidal configuration, Chem. Eng. J. 86 (2002) 83–85.

[7] M.R. Queiroz, S.A. Nebra, Theoretical and experimental analysis of the drying kinetics of bananas, J. Food Eng. 47 (2001) 127–132.

[8] R.G. Bowrey, K.A. Buckle, I. Hamey, P. Pavenayotin, Use of solar energy for banana drying, Food Technol. Australia 32 (6) (1980) 290–291.

[9] A.E. Drouzas, H. Schubert, Microwave application in vacuum drying of fruits, J. Food Eng. 28 (1996) 203–209.

[10] C.T. Kiranouidis, E. Tsami, Z.B. Maroulis, D. Marinos-Kouris, Drying kinetics of some fruits, Drying Technol. 15 (5) (1997) 1399–1418.

[11] S. Prasertsan, P. Saen-sabv, Heat pump drying of agricultural materials, Drying Technol. 16 (1–2) (1998) 235–250.

[12] P. Schirmer, S. Janjai, A. Esper, R. Smitabhindu, W. Muhhlbauer, Experimental investigation of the performance of the solar tunnel drying of bananas, Renewable Energy 7 (2) (1996) 119–129.

[13] M.K. Krokida, Z.B. Maroulis, Effect of drying method on shrinkage and porosity, Drying Technol. 15 (10) (1997) 2441–2458.

[14] K. Suzuki, K. Kubota, T. Hasegawa, H. Hosaka, Shrinkage in dehydration of root vegetables, J. Food Sci. 41 (1976) 1189–1193.

[15] W. Jomma, J.R. Puiggali, Drying of shrinkage materials: modeling with shrinkage velocity, Drying Technol. 9 (5) (1991) 1271–1293.
[16] V. Gekas, Y. Motarjemi, I. Lamgerg, B. Hallstrom, Evaluation of diffusion coefficients in a shrinking system, in: S. Bruin (Ed.), Preconcentration and Drying of Food Materials, Elsevier Science Publishers BV, Amsterdam, 1988.
[17] H. Desmorieux, C. Moyne, Analysis of dryer performance for tropical foodstuffs using the characteristic drying curve concept, in: A.S. Mujumder, (Ed.), Drying'92, 1992, pp. 834–843.
[18] Z. Qing, A mathematical model for drying of products undergoing shrinkage. M. Eng. thesis, National University of Singapore, 1997.
[19] A.F. Mills, Basic heat and mass transfer, IRWIN, MA, 1995.
[20] D.A. Van Meel, Adiabatic convection batch drying with recirculating air, Chem. Eng. Sci. 9 (1958) 36–44.
[21] N.N. Mohaimen, Thermal Properties of Food and Agricultural Products, G&B Publication, NY, 1980.
[22] M.A. Rao, S.S.H. Rizvi, Engineering Properties of Foods, Marcel Dekker, Inc., New York, 1986.
[23] M.A. Karim, M.N.A. Hawlader, Development of solar air collectors for drying applications, Energy Convers. Manage. 45 (2004) 329–344.
[24] M.N.A. Hawlader, M.S. Uddin, J.C. Ho, A.B.W. Teng, Drying characteristics of tomatoes, J. Food Eng. 14 (1991) 259–268.
[25] M. Balaban, G.M. Pogott, Mathematical model of simultaneous heat and mass transfer in food with dimensional changes and variable transport parameters, J. Food Sci. 53 (1988) 935–939.